

CHEMISTRY

A European Journal

A Journal of



Accepted Article

Title: An Unsaturated Four-Coordinate Dimethyl Dimolybdenum Complex with a Molybdenum-Molybdenum Quadruple Bond

Authors: Natalia Curado, Mario Carrasco, Jesus Campos, Celia Maya, Amor Rodríguez, Eliseo Ruiz, Santiago Alvarez, and Ernesto Carmona

This manuscript has been accepted after peer review and appears as an Accepted Article online prior to editing, proofing, and formal publication of the final Version of Record (VoR). This work is currently citable by using the Digital Object Identifier (DOI) given below. The VoR will be published online in Early View as soon as possible and may be different to this Accepted Article as a result of editing. Readers should obtain the VoR from the journal website shown below when it is published to ensure accuracy of information. The authors are responsible for the content of this Accepted Article.

To be cited as: *Chem. Eur. J.* 10.1002/chem.201604618

Link to VoR: <http://dx.doi.org/10.1002/chem.201604618>

Supported by
ACES

WILEY-VCH

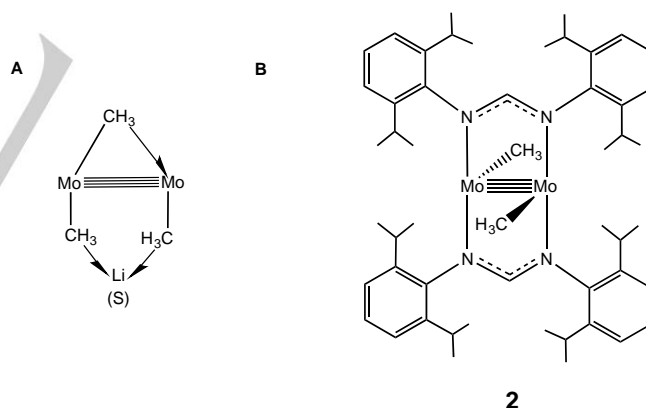
An Unsaturated Four-Coordinate Dimethyl Dimolybdenum Complex with a Molybdenum-Molybdenum Quadruple Bond

Natalia Curado^[a], Mario Carrasco^[a], Jesús Campos^[a], Celia Maya^[a], Amor Rodríguez^[a], E. Ruiz^[b], S. Álvarez^[b] and Ernesto Carmona^{*[a]}

We wish to dedicate this paper to Professor Carlo Mealli, for his contributions to the advancement of inorganic and organometallic chemistry.

Abstract: We describe the synthesis, molecular, and electronic structure of the complex $[\text{Mo}_2\text{Me}_2\{\mu\text{-HC(NDipp)}_2\}_2]$ (**2**), that contains a dimetallic core with a Mo–Mo quadruple bond and features uncommon four-coordinate geometry and fourteen-electron count at each molybdenum atom (Dipp = 2,6-*i*-Pr₂C₆H₃). The coordination polyhedron approaches a square pyramid with one of the molybdenum atoms nearly co-planar with the basal square plane in which the coordination position *trans* with respect to the Mo–Me bond is empty. The other three sites contain two *trans* nitrogen atoms of different amidinate ligands and the methyl group. The second Mo atom occupies the apex of the pyramid and forms a Mo–Mo bond of length 2.080(1) Å, consistent with a quadruple bond. Compound **2** reacts with tetrahydrofuran (THF) and trimethylphosphine to yield the mono-adducts $[\text{Mo}_2\text{Me}(\mu\text{-Me})\{\mu\text{-HC(NDipp)}_2\}_2(\text{L})]$ (**3-THF** and **3-PMe₃**, respectively) with one terminal and one bridging methyl groups. In contrast, 4-dimethylaminopyridine (dmap) forms the bis-adduct $[\text{Mo}_2\text{Me}_2\{\mu\text{-HC(NDipp)}_2\}_2(\text{dmap})_2]$ (**4**), with terminally coordinated methyl groups. Hydrogenolysis of complex **2** leads to the bis(hydride) $[\text{Mo}_2\text{H}_2\{\mu\text{-HC(NDipp)}_2\}_2(\text{thf})_2]$ (**5-THF**) with elimination of CH₄. Computational, kinetic and mechanistic studies, that include the use of D₂, and of complex **2** labelled with ¹³C (99%) at the Mo–CH₃ sites, support the intermediacy of a methyl-hydride reactive species. A computational DFT analysis of the terminal and bridging coordination of the methyl group to the Mo≡Mo core is also reported.

alkyl and aryl complexes of the (Mo₂)⁴⁺ core that could be used as precursors for low-coordinate second-row organometal(II) species and for related hydride complexes. As a result of these efforts, a series of mono- and bis-terphenyl complexes $[\text{Mo}_2(\text{Ar}')(\text{O}_2\text{CR})_3]$ and $[\text{Mo}_2(\text{Ar}')_2(\text{O}_2\text{CR})_2]$, were obtained for different terphenyl ligands (Ar') and carboxylate groups. The new compounds displayed a Mo–Mo bond length close to ca. 2.10 Å, typical of a quadruple bond, and a coordinative and electronic unsaturation partially compensated by the existence of weak Mo–C_{arene} secondary interactions involving η¹ binding of a flanking aryl ring.^[1,2] Latterly, within the same line of research, uncommon lithium di- and trimethyl dimolybdenum(II) *ate* complexes in which the unprecedented trimetallic agostic structure **A** (S = Et₂O, THF) is stabilized by metal coordination to auxiliary pyridylamido (also called aminopyridinate) and amidinate ligands were also investigated.^[3]



Introduction

In the course of studies on binuclear molybdenum compounds with M–M quadruple bonds we became interested in preparing

Although the methyl group is the simplest alkyl function, it can adopt a variety of coordination modes in its interaction with transition metal centres. Thus, besides common terminal binding M–Me, it can perform a bridging role, M(μ-Me)M, generating a variety of structures^[4–7] that encompass the symmetrical pyramidal and the monohapto agostic binding forms depicted in Figure 1.^[8,9] Even though a large number of methyl complexes of molybdenum is presently known, information on compounds of this sort that contain the (Mo₂)⁴⁺ central unit is scarce.^[10]



[a] Dr. N. Curado, Dr. M. Carrasco, Dr. E. Álvarez, Dr. J. Campos, Dr. C. Maya, Dr. R. Peloso, Dr. A. Rodríguez, Dr. J. López-Serrano, Prof. Dr. E. Carmona.

Instituto de Investigaciones Químicas (IIQ), Departamento de Química Inorgánica and Centro de Innovación en Química Avanzada (ORFEO-CINQA).

Consejo Superior de Investigaciones Científicas (CSIC) and Universidad de Sevilla.

Avda. Américo Vespucio, 49, 41092 Sevilla, Spain.

E-mail: guzman@us.es

[b] Prof. Dr. E. Ruiz, Prof. Dr. S. Álvarez Departament de Química Inorgànica and Institut de Química Teòrica i Computacional, Universitat de Barcelona Martí i Franquès 1–11, 08028 Barcelona (Spain)

Supporting information for this article is given via a link at the end of the document. (Please delete this text if not appropriate)

FULL PAPER

WILEY-VCH

Figure 1. Half-arrow representations for non-agostic $\mu^{\text{sp}^3\text{C}} - \text{Me}$ (left) and monohapto agostic $\mu^{\text{H}} - \text{Me}$ (right) bridging methyl groups (see ref. 8).

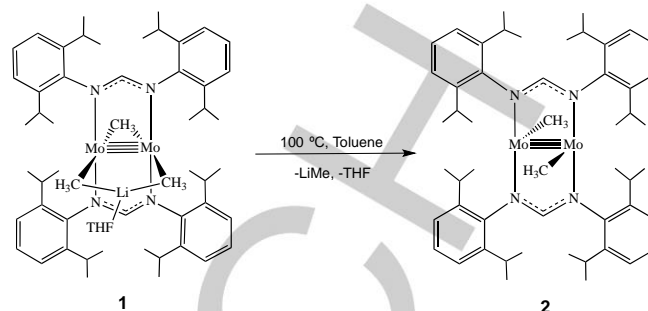
In 1974 the pyrophoric salt $[\text{Li}(\text{thf})_4][\text{Mo}_2\text{Me}_8]$ was prepared by Cotton, Wilkinson and co-workers and found to exhibit a Mo–Mo bond distance of 2.148(2) Å and Mo–Me bond lengths in the range ca. 2.27–2.31 Å.^[11] The structures of neutral complexes of composition $[\text{Mo}_2\text{Me}_4(\text{PR}_3)_4]$ ($\text{PR}_3 = \text{PMe}_3, \text{PMe}_2\text{Ph}$) were later ascertained with similar Mo–Mo (ca. 2.15 Å) and Mo–Me (2.25 Å) bond distances.^[12] No other methyl (Mo_2)⁴⁺ complexes seem to have been described with the exception of the mentioned *ate* complexes recently reported by our group, that were isolated as lithium derivatives with either contact ion pair or solvent-separated ion pair formulations. Some methyl derivatives with Mo–Mo bonds of order lower than four have also been described.^[13–16]

Transition metal organometallics that possess structures of low coordination number and low electron count are reactive species in a number of catalytic reactions.^[17] Furthermore, their unsaturated metal centres can provide active frames for the activation of small molecules such as H_2 ^[18] or N_2 ^[19]. In the field of molecular metal-metal multiple bonds, unusual physical properties and reactivity patterns have been disclosed in unsaturated complexes of chromium, molybdenum and other metals.^[20–25] In this article we report the synthesis and structure of the four-coordinate, fourteen-electron dimethyl complex $[\text{Mo}_2\text{Me}_2\{\mu\text{-HC}(\text{NDipp})_2\}_2]$ (**2**), that possesses the salient, unsaturated structure **B** (Dipp = 2,6-*i*-Pr₂C₆H₃). We also describe its reactivity towards Lewis bases such as THF, PMe_3 and 4-dimethylaminopyridine (dmap), along with the facile hydrogenolysis of its Mo–Me bonds. The latter reaction leads to the known^[26] bis(hydride) derivative $[\text{Mo}_2\text{H}_2\{\mu\text{-HC}(\text{NDipp})_2\}_2(\text{thf})_2]$ (**5**), through the intermediacy of the methyl-hydride species $[\text{Mo}_2(\text{CH}_3)(\text{H})\{\mu\text{-HC}(\text{NDipp})_2\}_2(\text{thf})_2]$ (**6·THF**). Kinetic, mechanistic and computational studies on this transformation are also provided.

Results and Discussion

As cited in the introductory comments, we have recently characterized some lithium trimethyl dimolybdenum(II) *ate* complexes that exhibit an unprecedented $\text{Li}(\mu\text{-Me})\text{Mo}(\mu\text{-Me})\text{Mo}(\mu\text{-Me})$ trimetallic core (structure **A**), supported by coordination to two bridging aminopyridinate or amidinate ligands. The amidinate derivative has composition $[\text{Mo}_2(\mu\text{-Me})\{\mu\text{-Me}\}_2\text{Li}(\text{THF})\{\mu\text{-HC}(\text{NDipp})_2\}_2]$ (**1**), and was obtained by the reaction of the bis(acetate)bis(amidinate) precursor $[\text{Mo}_2(\mu\text{-O}_2\text{CMe})_2\{\mu\text{-HC}(\text{NDipp})_2\}_2]$ (Dipp = 2,6-*i*-Pr₂C₆H₃) with an excess of LiMe. In some instances, NMR analysis of the reaction mixtures suggested the formation of small quantities of a lithium-devoid neutral methyl derivative, of the (Mo_2)⁴⁺ central unit. It was assumed that the new species contained a $[\text{Mo}_2\text{Me}_2]$ core, and accordingly, we set out to isolate this compound. We found that heating at 100 °C for 3–4 hours toluene or toluene-hexane solutions of **1** resulted in the elimination of LiMe and formation of the dimethyl complex **2** (Scheme 1). To avoid contamination by tetrahydrofuran (THF), that reacts instantly with **2** to yield the corresponding adduct **3·THF** (*vide infra*), solid **2** was treated twice with 5 mL of pentane, stirred for 15 min and thoroughly dried *in vacuo* (see

Experimental Section). Crystallization from toluene at -23 °C afforded very air sensitive red crystals of the desired product.



Scheme 1. Synthesis of unsaturated complex **2**.

Complex **2** did not react with either CO_2 (2 bar, 12 h, 25 °C) or C_2H_4 (0.5 bar, 12 h, 60 °C). In contrast, its treatment with LiMe at room temperature in a 1:1 molar ratio (Scheme 2) gave cleanly compound **1**, that was characterized by comparison of its NMR data with those of an authentic sample.^[3] New complexes formed when **2** was treated with an excess of THF, PMe_3 and 4-dimethylaminopyridine (dmap). While THF and PMe_3 yielded mono-adducts, **3·THF** and **3·PMe₃**, respectively, the pyridine-based ligand with smaller cone angle (101.1° for pyridine, vs 118° for PMe_3)^[27] afforded the bis(adduct) **4**. Under similar conditions, no observable reaction took place between complex **2** and the bulkier phosphine PMe_2Ph (cone angle 122°),^[27b] probably as a consequence of steric hindrance.

Complex **3·THF** was isolated as an oxygen- and moisture-sensitive red crystalline solid, following crystallization from a toluene:THF solvent mixture. As represented in Scheme 2, it converted back to the solvent free complex **2** by action of vacuum, at room temperature or slightly above (ca. 40 °C). Since the coordinated THF is highly labile (see below), **3·THF** was commonly used in place of **2** for many of the reactivity studies that will be discussed in the following paragraphs (see Scheme 2). The new complexes represented in Scheme 2 were characterized by microanalysis, NMR spectroscopy and X-ray crystallography. For the study of the reaction of **2** with H_2 , to be analysed in a forthcoming section, samples of this complex and of the adducts **3·THF** and **3·PMe₃** enriched in ¹³C (99%) at the Mo–CH₃ sites were prepared. Their examination by variable temperature NMR spectroscopy proved valuable for structural assignment. The ¹H NMR spectrum of complex **2** (C₇D₈, 25 °C) contains two septets (3.54 and 4.25 ppm) and four doublets (in the interval 1.0–1.4 ppm) for the eight *iso*-propyl substituents of the two amidinate ligands, consistent with the molecular symmetry proposed for this complex. In addition, a singlet at δ 1.89 can be attributed to the two equivalent Mo–CH₃ units. The corresponding ¹³C resonance appears at 14.7 ppm and is characterized by a ¹J_{CH} coupling constant of 120 Hz. These data are in agreement with terminal coordination of the methyl groups.^[3] Low temperature ¹³C{¹H} studies of complex **2** enriched in ¹³C were undertaken (Figure S1). Upon cooling at -20 °C the 14.7 ppm resonance broadens and fades into the base line when the temperature drops to -40 °C. Then it merges at -60 °C with δ 15.5 ppm, to become broader at -70 °C, and then disappear again into the base line when the temperature decreases to -85 °C. By comparison with the dynamic behaviour

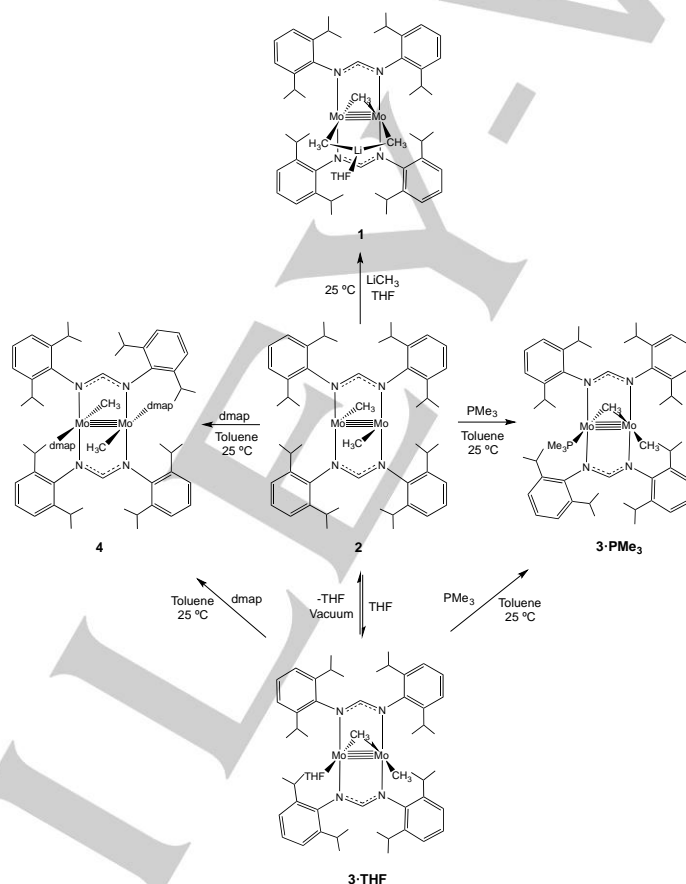
FULL PAPER

WILEY-VCH

of **3·THF** (*vide infra*) the higher energy dynamic process (coalescence temperature -40°C) can be attributed to equilibration of complex **2** with small, undetected amounts of its THF adduct (originated by minor amounts of THF). In turn, the lower energy process (coalescence at -85°C) could tentatively be viewed as involving an isomeric $\text{Mo}_2(\mu\text{-Me})_2$ bridging structure, although the lack of computational support in favour of this formulation (see below) casts doubts on the participation of such an species. An alternative possibility could be the attainment at very low temperatures of a weak ε -agostic interaction of the kind hinted by the X-ray data to be discussed in an upcoming section.

The ^1H NMR spectrum of **3·THF** (C_6D_6 , 25°C) shows only one resonance at 1.89 ppm attributable to the metal-bonded methyl protons, which is clearly in disagreement with the formulation presented in Scheme 2 that contains one terminal and one bridging methyl ligands. The corresponding ^{13}C NMR resonance appears with δ 15.9 and has a $^1J_{\text{CH}}$ coupling constant

of 118 Hz. Similarly, the *iso*-propyl substituents of the amidinate ligands of **3·THF** give rise to a pattern of signals that resembles that discussed above for the parent complex **2** (*i.e.* two septets at 3.81 and 4.04 ppm and four doublets in the range 1.0 – 1.4 ppm). All these data are in agreement with fast dissociation of the coordinated molecule of THF, a process that slows down considerably upon cooling at lower temperatures. Thus, only a broad hump centred at 16.1 ppm is observed at -20°C in the $^{13}\text{C}\{^1\text{H}\}$ NMR of a sample of **3·THF** enriched in ^{13}C (Figure S2) that becomes broader with further cooling, such that cannot be distinguished from the base line between -30 and -40°C . Extra cooling to -60°C causes, however, the appearance of three signals with chemical shifts 13.5, 15.5 and 21.2 ppm. The central one corresponds to complex **2**, whereas the other two can be respectively ascribed to the terminal and bridging methyl groups of complex **3·THF** by comparison with compound **3·PMe₃** (see below) and with other $\text{Mo}\equiv\text{Mo}$ complexes that contain terminal and bridging methyl groups.^[3]



Scheme 2. Reactivity of complex **2** toward different Lewis bases and generation of complexes **3·PMe₃** and **4** from **3·THF**.

As depicted in Scheme 2, the reaction of **2** or **3·THF** with PMe_3 (ca. 1.5 equiv) generated cleanly the analogous adduct **3·PMe₃** for which a similar structure containing terminal and bridging methyl groups can also be proposed. Notwithstanding, the room temperature ^1H , $^{13}\text{C}\{^1\text{H}\}$ and $^{31}\text{P}\{^1\text{H}\}$ NMR spectra feature broad resonances indicating that phosphine dissociation is fast under these conditions. Upon cooling at -45°C (C_7D_8) the

broad room temperature $^{31}\text{P}\{^1\text{H}\}$ NMR signal of **3·PMe₃** centred at -27 ppm converts into a sharp singlet with δ -23.4 . Similarly, two broad ^1H NMR resonances are recorded at -45°C with δ 0.25 and 1.37, due respectively to the terminal and bridging Mo-bonded methyl protons. The corresponding ^{13}C NMR signals appear at 17.5 ($^1J_{\text{CH}} = 115$ Hz) and 2.5 ppm ($^1J_{\text{CH}} = 115$ Hz; $^2J_{\text{CP}} = 40$ Hz). In the $^{13}\text{C}\{^1\text{H}\}$ NMR spectrum of ^{13}C -labelled **3·PMe₃**

FULL PAPER

WILEY-VCH

the $\text{Mo}(\mu\text{-}^{13}\text{CH}_3)\text{Mo}$ resonance appears as a doublet of doublets due to an additional $^2J_{\text{CC}}$ coupling of 5 Hz, whereas that due to the terminal $\text{Mo}\text{-}^{13}\text{CH}_3$ group (17.5 ppm) becomes somewhat broad, presumably, due to unresolved two-bond $^{13}\text{C}\text{-}^{13}\text{C}$, and three-bond $^{13}\text{C}\text{-}^{31}\text{P}$ couplings. These signals coalesce at 20°C (Figure S3; see the Supporting Information) and at 66°C give rise to a broad singlet centred in the proximity of 10.3 ppm. Using the slow-exchange approximation^[28] the rate constant at the coalescence temperature (ca. 293(±10)K) was calculated to be $k = 13060 (\pm 14) \text{ s}^{-1}$, with a corresponding ΔG^\ddagger value of 11.8 kcal·mol⁻¹. By contrast, the pyridine-derived adduct **4** contains two coordinated molecules of 4-dimethylaminopyridine and therefore two terminal $\text{Mo}\text{-Me}$ bonds. This complex was obtained employing either **2** or **3·THF** as precursors (Scheme 2). In contrast with the monoadducts **3·THF** and **3·PMe₃**, complex **4** has a rigid structure in solution under ambient conditions, the most distinctive NMR signals being the ^1H and ^{13}C resonances due to the equivalent $\text{Mo}\text{-CH}_3$ functions that appear respectively at 1.84 and 14.7 ppm. The latter exhibits a one-bond $^{13}\text{C}\text{-}^1\text{H}$ coupling constant of 120 Hz.

As already indicated, the neutral dimethyl complexes **2**, **3·THF**, **3·PMe₃** and **4** were characterized by single-crystal X-ray studies and their molecular structures are represented in Figures 2, 3, 4 and 5, respectively. Figure 2 contains two ORTEP perspective views of the molecules of **2** that emphasize their coordinative unsaturation. For each Mo atom the coordination polyhedron approaches closely a square pyramid in which one of the basal coordination sites (namely that *trans* relative to the $\text{Mo}\text{-CH}_3$ bond) is empty. The other three are occupied by two *trans* nitrogen atoms of different amidinate ligands and by the methyl group. Each Mo centre is nearly coplanar with its bonded donor atoms, although it is slightly displaced from this plane (by ca. 0.08 Å) toward the other molybdenum atom that occupies the apex of the pyramid. The $\text{Mo}\text{-Mo}$ bond distance of 2.080(1) Å is consistent with a metal-metal quadruple bond. The $\text{Me}\text{-Mo}\text{-Mo}$ bond angles (ca. 93°) and the $\text{Mo}\text{-Me}$ bond lengths (ca. 2.19 Å) are in accord with terminal coordination of the methyl groups.

As can also be seen in Figure 2 (bottom view) in the solid state two H atoms that belong to methyl groups of *iso*-propyl substituents of each amidinate ligand hover over the vacant coordination site of the molybdenum centres. The $\text{Mo}\cdots\text{H}$ distance is however long (2.7 Å) and the $\text{C}\text{-H}\cdots\text{Mo}$ angle large (149.5°). The two parameters are well above the range expected for agostic interactions (~1.8–2.3 Å and 90–140°).^[9] It therefore seems that complex **2** is a genuinely unsaturated, four-coordinate dimolybdenum complex and the marked unsaturation of its metal atoms is only compensated by weak ϵ -agostic interactions. This conclusion is in accordance with the solution NMR data already discussed. A three-coordinate quadruply bonded complex $[\text{Mo}_2(\mu\text{-}\eta^2\text{-Me}_2\text{Si}(\text{NDipp})_2)_2]$ has been reported. However, this compound exhibits a long $\text{Mo}\text{-Mo}$ quadruple bond (2.1784(12) Å) and fairly short $\text{Mo}\text{-N}$ bonds (1.958(4) Å) that are indicative of σ - and π -donor coordination behaviour of the amido nitrogen atoms.^[29]

The $(\text{Mo}_2)^{4+}$ core of adducts **3·THF**, **3·PMe₃** and **4** is characterized by a slightly longer $\text{Mo}\text{-Mo}$ bond of length in the range 2.086–2.110 Å, the longest distance (2.110(1) Å) corresponding to complex **4**. The $\text{Mo}_2(\mu\text{-N}^{\wedge}\text{N})_2$ framework that supports the coordinated methyl and neutral Lewis base ligands in these complexes ($\text{N}^{\wedge}\text{N}$ represents the amidinate ligand)

exhibits in all cases similar structural parameters that are also close to the corresponding metrics in **2**. Thus, $\text{Mo}\text{-N}$ distances range between 2.133(1) and 2.219(2) Å, *trans* $\text{N}\text{-Mo}\text{-N}$ bond angles have values of roughly 170° (between 164.85(6) and 177.04(6)°) and $\text{Mo}\text{-Mo}\text{-N}$ angles are of about 92° (between 91.09(6) and 94.20(6)°). Both kinds of bond angles are close to the ideal 180 and 90° values.

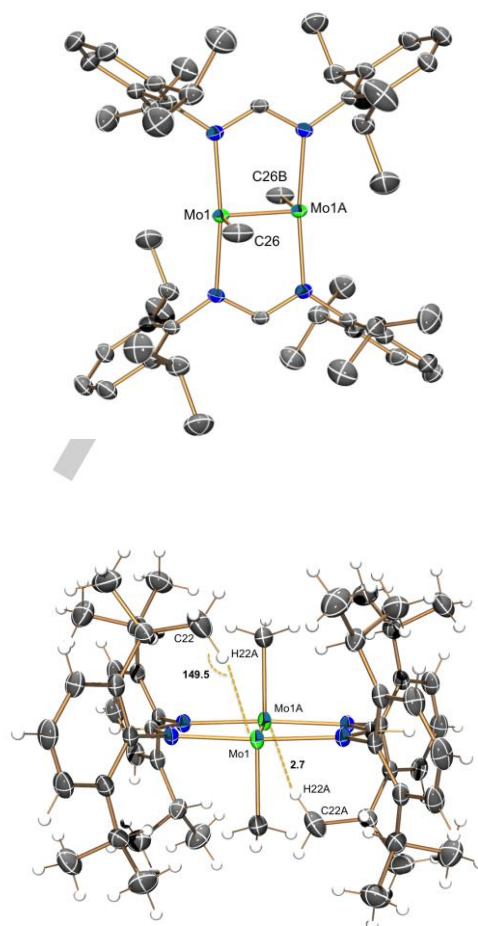


Figure 2. X-ray molecular structure of $[\text{Mo}_2\text{Me}_2(\mu\text{-HC}(\text{NDipp})_2)_2]$ (**2**), emphasizing the coordinative unsaturation of the Mo atoms (above) and the possible existence of weak ϵ -agostic interactions (bottom drawing). Anisotropic displacement parameters drawn at the 50% level. Selected bond lengths (Å) and angles (°): $\text{Mo}(1)\text{-Mo}(1\text{A})$, 2.080(1); $\text{Mo}(1)\text{-C}(26)$, 2.189(3); $\text{Mo}(1\text{A})\text{-Mo}(1)\text{-C}(26)$, 92.8(1).

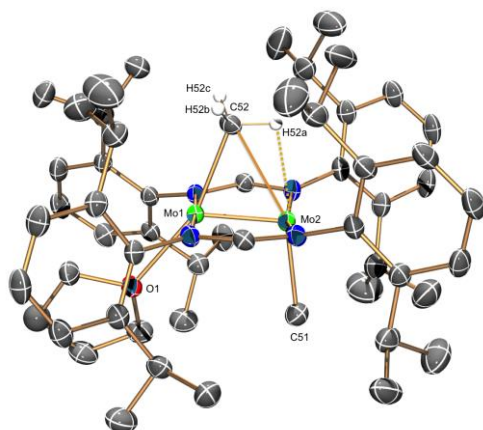


Figure 3. The solid state molecular structure of the tetrahydrofuran adduct $[\text{Mo}_2\text{Me}(\mu\text{-Me})\{\mu\text{-HC(NDipp)}_2\}_2(\text{THF})]$. Solid-state molecular structure of complex **3-THF** with thermal ellipsoids set at 50% probability. Some hydrogen atoms have been omitted for clarity. Selected bond lengths (Å) and angles (°): Mo(1)–Mo(2), 2.086(1); Mo(1)–O(1), 2.258(2); Mo(1)–C(52), 2.220(3); Mo(2)–C(52), 2.573(3); Mo(2)–C(51), 2.214(3); C(52)–Mo(1)–O(1), 160.4(1); C(52)–Mo(2)–C(51), 156.7(1); Mo(1)–C(52)–Mo(2), 51.0(1); O(1)–Mo(1)–Mo(2), 126.3(1); Mo(1)–Mo(2)–C(51), 101.0(1).

The two terminal Mo–CH₃ bonds of **4** have normal^[12–16] lengths (ca. 2.24 Å) although they are somewhat longer than the terminal Mo–CH₃ unit of **3-THF** (2.214(3) Å) and **3-PMe₃** (2.192(2) Å), perhaps as a consequence of the higher coordination number of the molybdenum atoms. However, in the latter two complexes there is a bridging methyl group that originates an acute Mo–C–Mo angle (approximately 51°, see Figures 3 and 4) and Mo–C bonds that differ appreciably in length. These Mo–C distances have values of 2.220(3) and 2.573(3) Å in **3-THF** and of 2.292(2) and 2.492(2) Å in the PMe₃ complex analogue. In each case the longer Mo2–C52 bond is approximately *trans* to the terminal Mo–C51 bond (C51–Mo2–C52 angles of 156.7(1) and 175.5(1)° for **3-THF** and **3-PMe₃**, respectively), and the difference between the shorter Mo–C bonds in the two complexes is doubtless due to the diverse *trans* influence exerted by the THF and PMe₃ ligands.^[30] The bond angle that at the pertinent Mo atom encompasses the terminal and bridging methyl groups in these complexes amounts 156.7(1) and 175.5(1)° in **3-THF** and **3-PMe₃**, respectively.

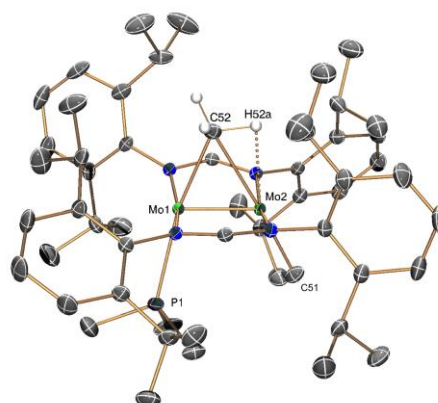


Figure 4. Solid-state molecular structures of complexes **3-PMe₃** with thermal ellipsoids set at 50% probability. Selected bond lengths (Å) and angles (°): Mo(1)–Mo(2), 2.088(1); Mo(1)–P(1), 2.591(1); Mo(1)–C(52), 2.292(2); Mo(2)–C(52), 2.492(2); Mo(2)–C(51), 2.192(2); C(52)–Mo(1)–P(1), 166.1(1); C(52)–Mo(2)–C(51), 175.5(1); Mo(1)–C(52)–Mo(2), 51.5(1); P(1)–Mo(1)–Mo(2), 102.3(1); Mo(1)–Mo(2)–C(51), 117.2(1).

Notwithstanding the uncertainties in defining the positions of hydrogen atoms by X-ray diffraction, the crystallographic data obtained for complexes **3** denote the existence in the solid state of a weak monohapto agostic interaction between the C52–H52A bond and the Mo2 atom (Figures 3 and 4). In addition to the already provided Mo2–C52 bond distances (2.573(3) and 2.492(2) Å), this three-centre two-electron interaction (3c-2e) is defined by a Mo2–H52A contact of about 2.28 Å and by a C–H–Mo angle of between ca. 96 and 87°, in the expected ranges for these parameters.^[9] Notice, however, that the Mo2–H52A separations are in the upper part of the 1.80–2.30 Å range considered for agostic interactions and furthermore that they are much longer than the Mo–H bonds in the bis(hydride) complex $[\text{Mo}_2\text{H}_2\{\mu\text{-HC(NDipp)}_2\}_2(\text{THF})_2]$ (**5-THF**) that have lengths of 1.71 Å.^[26] If one also takes into account that these bridging methyl groups present ¹J_{CH} couplings around 118 Hz, it can only be concluded that these agostic interactions must be weak.^[9,31]

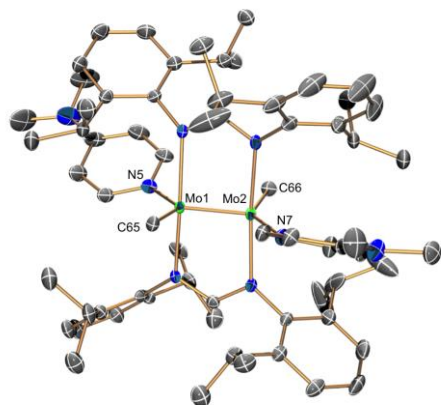
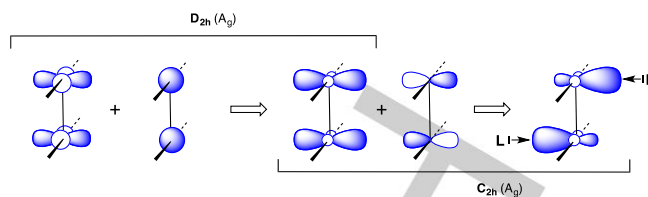


Figure 5. Solid-state molecular structure of compound **4** with thermal ellipsoids set at 50% probability. All hydrogen atoms have been omitted for clarity. Selected bond lengths (Å) and angles (°): Mo(1)–Mo(2), 2.110(1); Mo(1)–C(65), 2.236(2); Mo(2)–C(66), 2.247(2); Mo(1)–N(5), 2.321(2); Mo(2)–N(7), 2.302(2); C(65)–Mo(1)–Mo(2), 95.3(1); Mo(1)–Mo(2)–C(66), 91.9(1); N(5)–Mo(1)–Mo(2), 128.0(1); Mo(1)–Mo(2)–N(7), 124.3(1); N(5)–Mo(1)–C(65), 136.6(1); N(7)–Mo(2)–C(66), 143.6(1).

Geometry optimization of the base-free, *trans* complex **2**, (see Computational Details section), gave a structure in good agreement with the experimental one, with a terminal Me group bonded to each Mo atom. The *cis* isomer was found to correspond also to an energy minimum 5.8 kcal/mol higher in energy than the *trans* one. The lower stability of the *cis* isomer is most likely associated to steric repulsion between the two methyl groups, as suggested by Mo–Mo–Me bond angles of 104°, to be compared with 94° in the *trans* isomer. No energy minimum could be found for an alternative geometry with two bridging Me groups.

The special bonding topology of the quadruply bonded Mo₂Me₂(N[^]N)₂ preserves the Mo₂(N[^]N)₂ skeleton of the quintuply bonded precursor while the Mo atoms present an unusual square pyramidal coordination geometry with a vacant basal position (Figure 2). In the Mo^{II}₂(N[^]N)₂ fragment the bonding δ-type orbital that points in the direction of the N-donor ligands becomes the LUMO, which is allowed by symmetry to mix in some metal s orbital contribution (Scheme 3, D_{2h}(A_g)), thus hybridizing the d orbitals in the direction perpendicular to the Mo₂(N[^]N)₂ plane. Upon symmetry descent to that of the Mo₂Me₂(N[^]N)₂ complex (from D_{2h} to C_{2h}), further hybridization with metal p orbitals is possible, resulting in a fragment orbital with two lobes in the right directions to act as acceptors toward donor fragments. A similar hybridization scheme applies to the corresponding δ* orbital that yields an out-of-phase version of the acceptor orbital shown in Scheme 3, thus accounting for two possible donor-acceptor interactions with incoming ligands.



Scheme 3. Hybridization of d orbitals.

The calculated in-phase Mo–Me σ-bonding orbital, shown in Figure 6 clearly shows the hybridization expected from Scheme 3. Moreover, one can also observe some mixing-in of the σ-bonding combination of the z² orbitals that belongs to the same symmetry representation. A similar mixing of δ and σ metal-metal bonding components has already been detected in Cr–Cr quintuply bonded systems.^[32]

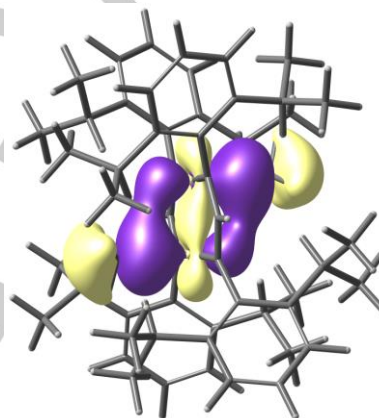


Figure 6. A_g molecular orbital incorporating Mo–Mo δ+σ and Mo–Me σ bonding character.

Reactivity of Complexes **2** and **3**·THF toward dihydrogen

Complexes **2** (plus added THF) and **3**·THF reacted cleanly at room temperature with H₂ (1.5 bar) in toluene, with elimination of CH₄, to afford the known bis(hydride) [Mo₂H₂{μ-HC(NDipp)₂}(thf)₂] (**5**·THF), in essentially quantitative yield (by ¹H NMR spectroscopy). In contrast, no reaction was observed between CH₄ and complex **2** enriched in ¹³C (99%) at the Mo–CH₃ sites, at temperatures of 60–80°C, and a pressure of 40 bar of methane.

To investigate the mechanism of the hydrogenolysis reaction, a kinetic study was carried out. Initially, adduct **3**·THF containing small amounts of tetrahydrofuran was utilized as a surrogate for **2**. Using ¹H NMR spectroscopy, the reaction rate was determined in C₇D₈ at 0°C under the pseudo-first-order conditions created by a dihydrogen pressure of 5 bar. A graphical concentration vs. time representation (Figure S4; see the Supporting Information) indicated not only first-order dependence on the concentration of **3**·THF, further confirmed by the straight line plot of the logarithmic function ln[**3**·THF] vs. time (Figure S5), but also the appearance of an intermediate, **6**·THF, that reached maximum concentration approximately upon completion of the first half-life (ca. 40 min) and subsequently

FULL PAPER

WILEY-VCH

decayed into product **5·THF** (Scheme 4). It was therefore clear that the overall transformation consisted of two consecutive irreversible pseudo-first-order reactions, of which the first was somewhat slower than the second. A computer fit of experimental data to theoretically predicted consecutive rate constants led to approximate $k_{\text{obs}1}$ and $k_{\text{obs}2}$ values of 3×10^{-4} and $8 \times 10^{-4} \text{ s}^{-1}$, respectively. It seems reasonable to propose that the reactive intermediate **6·THF** has a methyl-hydride formulation, $[\text{Mo}_2(\text{Me})(\text{H})]$, and this hypothesis was confirmed by mechanistic studies to be described below (Scheme 4).

To avoid the unnecessary kinetic complications due to coordinated THF in the above study of dihydrogen activation, a kinetic analysis of the analogous transformation of the Lewis base-free complex **2** was undertaken. Once more, reaction rates were measured in C_7D_8 under pseudo-first-order conditions over a H_2 pressure in the interval from 5 to 9 bar. Graphical representations of $\ln[2]$ vs. time (Figure S6) yielded straight lines in accordance with first-order dependence on the concentration of **2**. Furthermore, a plot of the observed rate constants against the concentration of H_2 was also linear (Figure 7A), indicating that the reaction was also first-order in dihydrogen. The concentration of dihydrogen in the samples was determined using ferrocene as an internal reference. The variation of k as a function of the reaction temperature was ascertained over the temperature range 15 to 35°C . An Eyring representation (Figure 7B) provided values of the activation parameters $\Delta H^\ddagger = 12.5(1.7) \text{ kcal}\cdot\text{mol}^{-1}$, $\Delta S^\ddagger = -28.0(5.9) \text{ cal}\cdot\text{mol}^{-1}\cdot\text{K}^{-1}$, with $\Delta G^\ddagger = 20.9(0.2) \text{ kcal}\cdot\text{mol}^{-1}$. Besides, use of D_2 (Figure S7) provided a kinetic isotope effect $k_{\text{H}}/k_{\text{D}}$ of 2.9, indicating that cleavage of the H–H bond was rate determining.

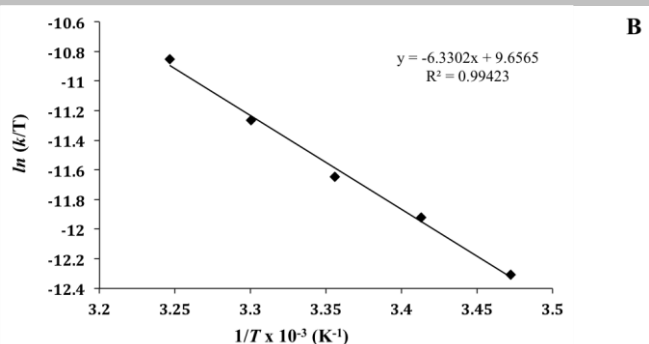
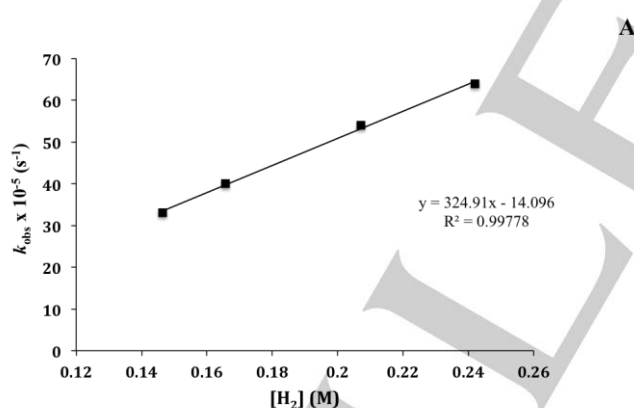
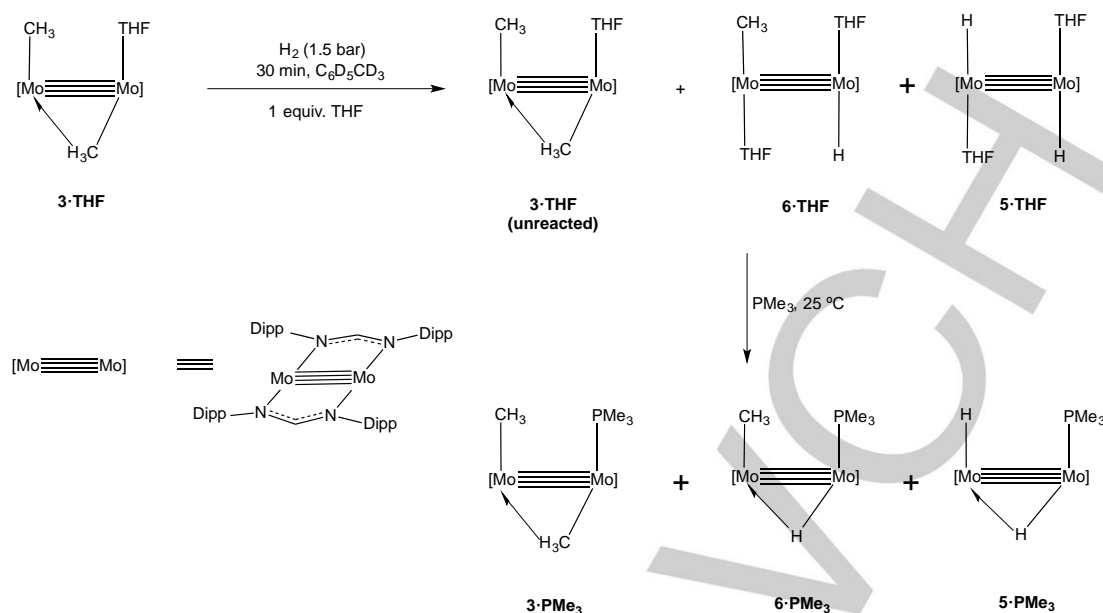


Figure 7. Plot of pseudo-first-order rate constant (k_{obs}) vs. H_2 concentration (A) and Eyring representation (B) for the hydrogenolysis of complex **2**.

To gain information on the nature of the reaction intermediate, further experimental work was accomplished. The purported hydride-methyl species was also detected in the reaction of **2** with H_2 although it was more difficult to observe due to faster reaction rates in comparison with **3·THF**. Accordingly, the latter complex was utilised for these studies that were performed in an NMR tube with C_7D_8 as the solvent.

Treatment of a C_7D_8 solution of **3·THF** with 1.5 bar of H_2 produced after ca. 30 min at 25°C a mixture of unreacted **3·THF**, the bis(hydride) product **5·THF** and the hydride-methyl complex **6·THF** (Scheme 4) in an approximate 2:1:1 ratio. The reaction was quenched by removal of H_2 , and a slight excess of PMe_3 (ca 1.5 equiv. relative to **3·THF**) was added at 25°C , to convert the above mixture of products into the corresponding PMe_3 adducts, **3·PMe₃**, **5·PMe₃** and **6·PMe₃**. The complete experiment was repeated utilising D_2 instead of H_2 , and furthermore the **3·PMe₃**: **5·PMe₃**: **6·PMe₃** mixture was also engendered starting from **3·THF** enriched in ^{13}C (99%) at the Mo–CH₃ sites. For experimental convenience, to avoid overlap of signature resonances, ^1H and ^{31}P NMR identification of the aforementioned mixtures was effected at -10°C , whereas ^{13}C NMR spectra were measured at 0°C .

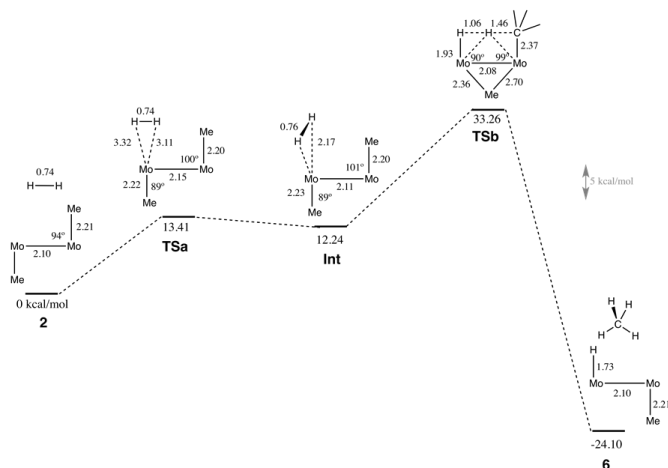


Scheme 4. Products of the NMR-tube reaction of **3-THF** and H_2 quenched after ca. 50% conversion and generation of the corresponding PMe_3 adducts. The 3c-2e interactions are depicted using the half-arrow notation proposed by Green, Green and Parking.^[8] The bridging amidinate ligands have been omitted for the sake of clarity.

Identification of the individual components of the foregoing mixtures of products by multinuclear NMR spectroscopy was straightforward. Thus complexes **3-THF**, **3-PMe3**, **5-THF** and **5-PMe3** (in the pertinent isotopologue forms) were authenticated by comparison of their NMR parameters with those of authentic samples.^[26a,33] Signature NMR data for the pursued intermediates **6-THF** and **6-PMe3** provided strong support for the hydride-methyl formulation proposed in Scheme 4. Particularly noteworthy are the following: (i) A ^{31}P NMR resonance at -10°C for **6-PMe3** characterized by $\delta -12.7$, $^2J_{\text{PH}} = 60$ and $^2J_{\text{PD}} = 9$ Hz. (ii) The Mo-CH₃ group of **6-PMe3** is responsible for a ^{13}C resonance at ca. 17 ppm that exhibits $^1J_{\text{CH}}$, $^3J_{\text{CH}}$ and $^3J_{\text{CP}}$ coupling constants of 116, 18 and 2 Hz, respectively. In **6-THF** enriched in ^{13}C this signal appears at 18.2 ppm although an additional $^3J_{\text{CH}}$ coupling with the hydride ligand of 17 Hz becomes discernable ($^1J_{\text{CH}} = 115$ Hz). (iii) The Mo-H resonance of **6-THF** appears at 6.23 (ca. 6.1 ppm in the deuterated isotopologue). This chemical shift is very close to that recorded for the bis(hydride) complex **5-THF** (5.7 ppm; ca. 5.8 ppm for the bis-deuteride isotopologue).

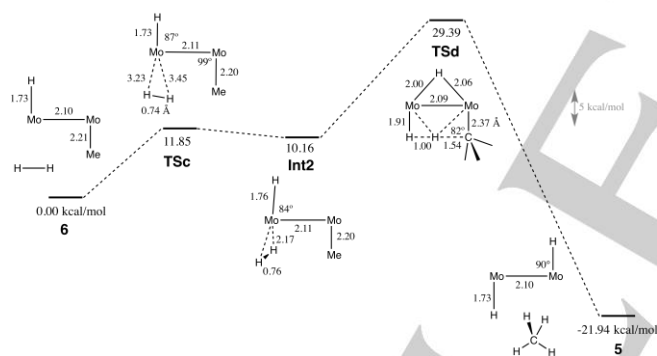
A detailed mechanism for the hydrogenation reaction of **2** can be obtained from a computational study of stationary points along the potential energy surface along a path that takes from **2** to **6**. The species that have been found as stationary points along such path, their relative energies and some relevant bond distances and angles are shown in Scheme 5. The approach of H_2 to the dimolybdenum species **2** yields a transition state (**TS1**) with a side-on orientation relative to a Mo atom. This transition state corresponds to the point at which H_2 passes in between three Me groups, two from the aryl groups of the amidinate ligands coordinated to the Mo atom being approached, and the Me group coordinated to the other Mo atom (seven H-H...H-C distances between 2.31 and 2.59 Å). Then it proceeds to an intermediate (**Int**) with a σ -bond coordinated H_2 , with the H-H

and Mo-Mo bonds perpendicular to each other. Then, rotation of H_2 forms an incipient H-C bond with a methyl group, while the other Me adopts a bridging coordination mode in a transition state (**TS2**). The next step seems to consist in a concerted bond reorganization that results in the liberation of a methane molecule and the transfer of the other methyl group to the non-hydrogenated Mo atom to give the detected intermediate **6**. The free energy change for this whole process is -24.1 kcal/mol. The rate determining step is the formation of the **TS2** transition state that involves significant lengthening of the Mo-Me bond to the leaving methyl group, and partial formation of a new H-Me bond. The calculated barrier appears of magnitude somewhat disproportionate to the observed kinetics, though it is most probably overestimated by the B3LYP functional used.^[34] Besides, the computed mechanism is consistent with the described kinetics studies and reaction rate dependence with the partial pressure of H_2 . Application of the dispersion correction B3LYP method to the stationary states did not modify appreciably the energy barriers. A final point of note in this regard is that this barrier is lower than calculated for an alternative path discussed below implying axial attack of H_2 to the Mo-Mo quadruple bond.



Scheme 5. Stationary points along hydrogenation reaction of **2** and their relative free energies. Some relevant bond distances and angles are also shown.

Subsequent hydrogenation of **6** follows a similar path (Scheme 6), the main qualitative difference being that in the rate determining transition state (**TS4**) there is now a bridging hydride instead of the bridging methyl in **TS2**. The relative energies of the two transition states, the intermediate and the final product are similar to those of the first hydrogenation, if slightly lower. Again in this second reaction, the rate determining step implies the activation of the Mo–Me and H–H bonds.



Scheme 6. Stationary points along subsequent hydrogenation reaction of **6** and their relative free energies. Some relevant bond distances and angles are also shown.

An alternative reaction path was computationally analyzed, in which the dihydrogen molecule attacks the molybdenum atom perpendicularly to the Mo–Mo bond, but the calculated energy barriers are higher than for the pathway just discussed: 47.4 and 49.4 kcal/mol for the first and second hydrogenation steps, respectively (see Electronic Supporting Information, Figures S21 and S22). Despite these efforts, we cannot discard the possibility of an unforeseen mechanism, different from the two considered here, may be operative.

Conclusions

The computational, crystallographic and NMR studies described in this paper underscore that although terminal and bridging coordination of methyl groups to a quadruply bonded Mo₂ core have comparable energetics, the former is preferred to the latter. This appears to be a common situation that applies widely to other metal-metal bonded transition metal complexes.^[14a, 35–38] In the context of the work reported herein, it explains the observation in the solid state of the four-coordinate, fourteen-electron structure of complex **2**, in spite of its marked unsaturation, clearly manifested in its reactivity toward conventional Lewis bases and against dihydrogen.

Experimental Section

General considerations.

All manipulations were carried out using standard Schlenk and glove-box techniques, under an atmosphere of argon and of high purity nitrogen, respectively. All solvents were dried, stored over 4 Å molecular sieves, and degassed prior to use. Toluene (C₇H₈), *n*-pentane (C₅H₁₂) and *n*-hexane (C₆H₁₄) were distilled under nitrogen over sodium. Tetrahydrofuran (THF) and diethyl ether were distilled under nitrogen over sodium/benzophenone. [D₆]Benzene and [D₈]THF were distilled under argon over sodium/benzophenone; [D₈]toluene was distilled under argon over sodium. The quadruply bonded complex [Mo₂(μ-Me)(μ-Me)₂Li(thf){μ-HC(NDipp)₂}₂] (**1**) was prepared as described previously.^[3] Solution NMR spectra were recorded on Bruker AMX-300, DRX-400 and DRX-500 spectrometers. Spectra were referenced to external SiMe₄ (δ: 0 ppm) using the residual proton solvent peaks as internal standards (¹H NMR experiments), or the characteristic resonances of the solvent nuclei (¹³C NMR experiments), while ³¹P was referenced to H₃PO₄. Spectral assignments were made by routine one- and two-dimensional NMR experiments (¹H, ¹³C, ¹³C{¹H}, ³¹P{¹H}, COSY, NOESY, HSQC and HMBC) where appropriate. UV–visible spectra were recorded on a Perkin Elmer Lambda 750 spectrometer. For elemental analyses a LECO TruSpec CHN elementary analyzer, was utilized. Crystals of compounds **2**, **3-PMe**, **3-THF** and **4** were mounted in oil on glass fibers and fixed in a cold nitrogen stream. Data were measured on a Bruker APEX II CCD diffractometer equipped with Ag-K_α radiation and graphite monochromator and processed with APEX-W2D-NT (Bruker, 2004), cell refinement and data reduction with SAINT-Plus (Bruker, 2004) and the absorption was corrected by multiscan method applied by SADABS. The structures of the three samples were determined by the direct method routines in the SHELXS program and refined by full-matrix least-squares methods on F², in SHELXL-97.^[39] The non-hydrogen atoms were refined anisotropically. Except for H13, H38 and H52 hydrogens of compound **3-THF** which were refined freely, all hydrogen atoms were included in idealised positions and their U_{iso} values were set to ride on the U_{eq} values of the parent carbon atoms. A summary of the fundamental crystal and refinement data are given in the Tables S8–11 of the Supporting Information. Atomic coordinates, anisotropic displacement parameters and bond lengths and angles can be found in the cif files. Crystallographic data have been deposited in the Cambridge Crystallographic Data Centre with no. 1449191–1449194. These data can be obtained free of charge from The Cambridge Crystallographic Data Centre via www.ccdc.cam.ac.uk/data_request/cif

Synthesis of [Mo₂(Me)₂{μ-HC(NDipp)₂}₂] (**2**)

The complex [Mo₂(μ-Me){(μ-Me)₂Li(THF)}{μ-HC(NDipp)₂}₂] (**1**), was generated from [Mo₂(μ-O₂CMe)₂{μ-HC(NDipp)₂}₂] and LiMe as described previously.^[3] A solution of **1** in toluene (0.8 g, ca. 0.6 mmol, 15 mL) was

FULL PAPER

WILEY-VCH

heated at 100°C for 3 hours and it was then cooled down to room temperature, filtered and evaporated to dryness. Pentane (2 x 5 mL) was added and the resulting suspension was stirred at room temperature for 15 min before removal of the solvent. The red-brown solid that was obtained was further dried under vacuum for 1 h and re-dissolved in toluene (ca. 0.5 g of the complex in 10 mL of the solvent) with warming at around 60°C. The resulting concentrated solution was kept at -23°C for two days to give red crystals of complex **2** (0.2 g, 42%). ¹H NMR (400 MHz, C₆D₆, 25°C): δ = 1.01, 1.16, 1.26, 1.37 (d, 12H each, ³J_{HH} = 6.7 Hz, Me_{Dipp}), 1.89 (s, 6H, Mo-Me₁), 3.54, 4.25 (sept, 4H each, ³J_{HH} = 6.7 Hz, CHMe₂), 6.92 (dd, 4H, ³J_{HH} = 7.5 Hz, ⁴J_{HH} = 1.2 Hz, *m*-Dipp), 7.03 (apparent t, 4H, ³J_{HH} = 7.5 Hz, *p*-Dipp), 7.09 (dd, 4H, ³J_{HH} = 7.5 Hz, ⁴J_{HH} = 1.2 Hz, *m'*-Dipp), 8.31 ppm (s, 2H, NC(H)N). The signal ' designs the groups closer to the methyl group (Mo-CH₃). ¹³C{¹H} NMR (100 MHz, C₆D₆, 25°C): δ = 14.7 (s, Mo-Me₁), 25.0, 25.1, 25.3, 26.0 (Me_{Dipp}), 28.3, 29.7 (CHMe₂), 123.5 (*m*-Dipp), 124.9 (*m'*-Dipp), 126.3 (*p*-Dipp), 143.9 (*o'*-Dipp), 144.9 (*o*-Dipp), 145.4 (*ipso*-Dipp), 161.6 ppm (NC(H)N). The signal ' designs the groups closer to the methyl group (Mo-CH₃). ¹³C, ¹H NMR (100 MHz, C₆D₆, 25°C): δ = 14.7 ppm (q, ¹J_{CH} ~ 120 Hz, Mo-Me₁). Elemental analysis calcd. (%) for C₅₂H₇₆Mo₂N₄: C, 65.81; H, 8.07; N, 5.90. Expt.: C, 66.0; H, 8.4; N, 6.1.

Synthesis of [Mo₂(μ-Me)(Me){μ-HC(NDipp)₂}(thf)] (3-THF)

Procedure A. Red crystals of the title complex were obtained from a saturated solution of complex **2** (0.6 g) in a mixture of toluene (7 mL) and THF (0.3 mL) at -23°C for 2 days (310 mg, 48%). **Procedure B.** A solution of complex **1** (2.0 g, 1.6 mmol) in toluene (30 mL) was heated at 100°C for 3 hours. The reaction mixture was filtered and the red solution was dried under vacuum (340 mg, 67%). ¹H NMR (400 MHz, C₆D₆, 25°C): δ = 1.08, 1.15 (d, 12H each, ³J_{HH} = 6.8 Hz, Me_{Dipp}), 1.26 (m, 4H, O-CH₂CH₂), 1.33, 1.36 (d, 12H each, ³J_{HH} = 6.8 Hz, Me_{Dipp}), 1.89 (s, 6H, Mo-Me₁), 3.39 (m, O-CH₂CH₂), 3.81, 4.04 (sept, 4H each, ³J_{HH} = 6.8 Hz, CHMe₂), 6.98-7.06 (m, *m*-Dipp, *m'*-Dipp, *p*-Dipp), 8.28 ppm (s, 2H, NC(H)N). ¹³C{¹H} NMR (100 MHz, C₆D₆, 25°C): δ = 15.9 (s, Mo-Me₁), 24.9, 25.0 (Me_{Dipp}), 25.7 (O-CH₂CH₂), 26.3, 26.7 (Me_{Dipp}), 28.5, 28.7 (CHMe₂), 68.2 (O-CH₂CH₂), 124.1, 124.2 (*m*-Dipp), 126.0 (*p*-Dipp), 144.5, 145.0 (*o*-Dipp), 145.9 (*ipso*-Dipp), 162.0 ppm (NC(H)N). The signal ' designs the groups closer to the methyl group (Mo-CH₃). ¹³C, ¹H NMR (100 MHz, C₆D₆, 25°C): δ = 15.9 ppm (q, ¹J_{CH} ~ 118 Hz, Mo-Me₁). UV-Visible (C₆D₆): λ_{max} (ε) = 480 nm (2160 mol⁻¹ L cm⁻¹). Elemental analysis calcd. (%) for C₅₆H₈₄Mo₂N₄O: C, 65.87; H, 8.29; N, 5.49. Found: C, 66.0; H, 8.4; N, 5.7.

Synthesis of [Mo₂(μ-Me)(Me){μ-HC(NDipp)₂}(PMe₃)] (3-PMe₃)

About 0.5 mmol of either compound **2** or **3-THF** was dissolved in toluene (10 mL) and PMe₃ was added dropwise (1.5 equiv) to the solution mixture. After 2 hours of stirring at room temperature the solvent was evaporated *in vacuo*, and the resulting solid was washed with pentane (5 mL) at 0°C. Crystals were obtained from a saturated solution of the complex in toluene at -23°C for 24 hours (340 mg, 67%). ¹H NMR (500 MHz, C₇D₈, -45°C): δ = 0.25 (s, 3H, Mo-Me₁), 0.45, 0.67 (d, 6H each, Me_{Dipp}), 0.95 (m, 9H, PMe₃), 0.97, 1.06, 1.17 (s, 6H each, Me_{Dipp}), 1.22 (m, 9H, Mo-μ-Me y Me_{Dipp}), 1.32, 1.37 (s, 6H each, Me_{Dipp}), 3.40 (m, 4H, CHMe₂), 3.82, 3.93 (m, 2H each, CHMe₂), 6.8-7.07 (m, 12H, *m*-Dipp, *m'*-Dipp, *p*-Dipp), 8.67 ppm (s, 2H, NC(H)N). The signal ' designs the groups closer to the methyl group (Mo-CH₃). ¹³C{¹H} NMR (125 MHz, C₇D₈, -45°C): δ = 2.5 (d, ²J_{PC} = 40 Hz, μ-Me), 14.4 (d, ¹J_{PC} = 18 Hz, PMe₃), 17.5 (Mo-Me₁), 23.3, 23.5, 24.5, 24.6, 25.7, 26.8, 27.2, 27.4 (Me_{Dipp}), 26.7, 28.1, 28.2, 28.3 (CHMe₂), 123.4-125.6 (*m*-Dipp^a, *m'*-Dipp^a, *p*-Dipp^a, *m*-Dipp^b, *m'*-Dipp^b, *p*-Dipp^b), 141.2, 143.2, 143.3, 144.0 (*o*-Dipp), 145.8, 145.9 (*ipso*-Dipp), 162.5 ppm (NC(H)N). The signal ' designs the groups closer to the methyl group (Mo-CH₃). ¹³C, ¹H NMR (125 MHz, C₇D₈, -45°C): δ = 2.5 ppm (dq, ¹J_{CH} ~ 115 Hz, ²J_{PCtrans} = 40 Hz, μ-Me), 17.5 (q, ¹J_{CH} ~ 115 Hz, Mo-Me₁). ³¹P{¹H} NMR (200 MHz, C₇D₈, -45°C): δ = -23.4 ppm. The signals are broad due to the low temperature and the fluxionality of the complex. UV-Visible (C₆D₆): λ_{max} (ε) = 339, 390

(shoulders), 540 nm (1270 mol⁻¹ L cm⁻¹). Elemental analysis calcd. (%) for C₅₅H₈₅Mo₂N₄P: C, 64.44; H, 8.36; N, 5.47. Found: C, 64.5; H, 8.8; N, 5.9.

Synthesis of [Mo₂(Me)₂{μ-HC(NDipp)₂}(dmap)₂] (4)

Starting from complex **2** or **3-THF** (ca. 0.2 mmol) and 4-dimethylaminopyridine (0.06 g, 0.5 mmol) a toluene solution was prepared (10 mL) and stirred at room temperature for 5 hours. Concentration of the solvent gave a bright red solid that was crystallized from a saturated toluene solution after cooling at -23°C for 3 days (160 mg, 65%). ¹H NMR (500 MHz, C₆D₆, 25°C): δ (ppm): 1.03, 1.18, 1.30, 1.46 (d, 12H each, ³J_{HH} = 7.1 Hz, Me_{Dipp}), 1.84 (s, 6H, Mo-Me₂), 2.1(s, 12H, pyr-NMe₂), 3.91, 4.04 (sept, 4H each, ³J_{HH} = 6.2 Hz, CHMe₂), 5.89 (broad s, 4H, 3,5-pyr), 6.99-6.93 (m, 8H, *m'*-Dipp, *p*-Dipp, *p*-Dipp), 7.01 (dd, 4H, ³J_{HH} = 7.4 Hz, ⁴J_{HH} = 2.6 Hz, *m*-Dipp), 8.01 (broad s, 4H, 2,6-pyr), 8.37 ppm (s, 2H, NC(H)N). The signal ' designs the groups closer to the methyl group (Mo-CH₃). ¹³C{¹H} NMR (125 MHz, C₆D₆, 25°C): δ (ppm): 14.7 (Mo-Me), 24.3, 24.4, 26.3, 27.5 (CHMe₂), 27.8, 28.0 (CHMe₂), 37.9 (pyr-NMe₂), 106.4 (3,5-pyr), 123.0 (*m*-Dipp), 123.7 (*p*-Dipp, *p*-Dipp), 124.9 (*m'*-Dipp), 144.5, 144.7 (*o*-Dipp, *o*-Dipp), 146.5 (*ipso*-Dipp), 149.2 (2,4-pyr), 153.7 (*ipso*-pyr-NMe₂), 161.4 ppm (NC(H)N). The signal ' designs the groups closer to the methyl group (Mo-CH₃). ¹³C, ¹H NMR (125 MHz, C₆D₆, 25°C): δ (ppm): 14.7 ppm (q, ¹J_{CH} ~ 120 Hz, Mo-Me). UV-Visible (C₆D₆): λ_{max} (ε) = 360, 440 (shoulders), 512 nm (3150 mol⁻¹ L cm⁻¹). Elemental analysis calcd (%) for C₆₄H₈₂Mo₂N₈: C, 66.42; H, 8.11; N, 9.39. Found: C, 66.0; H, 8.6; N, 9.6.

Reactions of complexes **2** and **3-THF** with H₂

Complex 2. Complex **2** (2 mg, 2x10⁻³ mmol) was dissolved in 0.45 mL of C₇D₈. To this solution, 0.1 mL of the standard solution of ferrocene in C₇D₈ (0.0215 M) was added. Three vacuum/argon cycles were performed at -70°C to remove the argon atmosphere in the Young NMR tube. For the different experiments performed, the tube was then charged with 5, 7, 8 or 9 bar of dihydrogen at -70°C and shaken (Figure S6). The reaction progress was checked by ¹H NMR spectroscopy at 25 °C. Analogous experiments were carried out with a fixed pressure of 8 bar of dihydrogen at 15, 20, 25, 30 and 35°C. To measure the kinetic isotope effect, two identical solutions of complex **2** in C₇D₈ were prepared (2 mg, 2x10⁻³ mmol). After cooling at -70°C, the argon atmosphere was pumped out and the corresponding NMR tubes were charged with a pressure of 5 bar of H₂ and D₂, respectively (see Figure S7).

Complex 3-THF. Complex **3-THF** (2.5 mg, 2.5 x 10⁻³ mmol) in 0.55 mL of C₇D₈ was cooled to -70°C. The argon atmosphere was pumped out and replaced by 4, 5 or 6 bars of H₂. The reaction progress was checked by ¹H NMR spectroscopy at 0°C.

Computational Details

The calculations were performed with the Gaussian09 computer code.^[40] The hybrid B3LYP functional^[41] was employed together with the all-electron triple-ζ basis set proposed by Schäfer *et al.*^[42] for the light atoms while for the molybdenum atoms an all-electron basis set with a contraction {84211111/6411111/51111} was used.^[43] This all-electron basis set was used to avoid problems found with common pseudopotentials that provide artifact charge and bond order values for the studied complexes. Transition states and energy minima were corroborated by the calculation of the corresponding frequencies.

Acknowledgements

Financial support (FEDER contribution) from the Spanish Ministry of Science and Innovation (Projects CTQ2010-15833, CTQ2013-42501-P, CTQ2014-52769-C3-3-R, CTQ2015-64579-

FULL PAPER

WILEY-VCH

C3-1-P and Consolider-Ingenio 2010 CSD2007-00006) and the Junta de Andalucía (Grant FQM-119 and Project P09-FQM-5117) is gratefully acknowledged. M.C. and N.C. thank the Spanish Ministry of Education (AP-4193) and the Spanish Ministry of Science and Innovation (BES-2011-047643) for research grants. J.C. thanks the EU 7th Framework Program, Marie Skłodowska-Curie actions (COFUND, Grant Agreement no. 267226) and Junta de Andalucía for a Talentia Postdoc Fellowship. E.R. thanks the Generalitat de Catalunya for an ICREA Academia grant. E.R. and S.A. thank the CSUC for computational resources. The group of Homegeneous Catalysis at CIQSO-University of Huelva (Spain) is gratefully acknowledged, in particular Professors P. J. Pérez and T. R. Belderrain, and Dr. J. M. Muñoz-Molina for facilities and assistance in high-pressure reactions. We are grateful to Professor Carmen Carmona, from the Department of Physical Chemistry of the University of Sevilla, for valuable assistance in the interpretation and computer simulation of kinetic results.

Keywords: Alkyl complexes • Dimolybdenum • Agostic interactions • Kinetics • Theoretical calculations

- [1] a) M. Carrasco, M. Faust, R. Peloso, A. Rodríguez, J. López-Serrano, E. Álvarez, C. Maya, P. P. Power, E. Carmona, *Chem. Commun.* **2012**, 48, 3954–3956; b) M. Carrasco, I. Mendoza, M. Faust, J. López-Serrano, R. Peloso, A. Rodríguez, E. Álvarez, C. Maya, P. P. Power, E. Carmona, *J. Am. Chem. Soc.*, **2014**, 136, 9173–9180.
- [2] M. Carrasco, I. Mendoza, E. Álvarez, A. Grirrane, C. Maya, R. Peloso, A. Rodríguez, A. Falceto, S. Álvarez, E. Carmona, *Chem. - A Eur. J.*, **2015**, 21, 410–421.
- [3] N. Curado, M. Carrasco, E. Álvarez, C. Maya, R. Peloso, A. Rodríguez, J. López-Serrano, and E. Carmona, *J. Am. Chem. Soc.*, **2015**, 137, 12378–12387.
- [4] For some review articles: (a) J. Holton, M. F. Lappert, R. Pearce, P. I. W. Yarrow, *Chem. Rev.*, **1983**, 83, 135–201; (b) P. Braunstein, N. M. Boag, *Angew. Chem., Int. Ed.*, **2001**, 40, 2427–2433; (c) J. Campos, J. López-Serrano, R. Peloso, E. Carmona, *Chem. Eur. J.*, **2016**, DOI 10.1002/chem.201504483.
- [5] a) J. W. Park, P. B. Mackenzie, W. P. Schaefer, R. H. Grubbs, *J. Am. Chem. Soc.*, **1986**, 108, 6402–6404; b) F. Ozawa, J. W. Park, P. B. Mackenzie, W. P. Schaefer, L. M. Henling, R. H. Grubbs, *J. Am. Chem. Soc.*, **1989**, 111, 1319–1327; c) P. B. Mackenzie, R. J. Coots, R. H. Grubbs, *Organometallics*, **1989**, 8, 8–14; d) C. P. Casey, P. J. Fagan, W. H. Miles, *J. Am. Chem. Soc.* **1982**, 104, 1134–1136; e) B. E. Bursten, R. H. Cayton, *Organometallics*, **1986**, 5, 1051–1053.
- [6] a) S. D. Stults, R. A. Andersen, A. Zalkin, *J. Am. Chem. Soc.*, **1989**, 111, 4507–4508; b) D. J. Schwartz, G. E. Ball, R. A. Andersen, *J. Am. Chem. Soc.*, **1995**, 117, 6027–6040; c) H. M. Dietrich, H. Grove, K. W. Tömmros, R. Anwender, *J. Am. Chem. Soc.*, **2006**, 128, 1458–1459.
- [7] a) M. Niemeyer, P. P. Power, *Chem. Commun.*, **1996**, 1573–1574; b) M. C. W. Chan, J. M. Cole, V. C. Gibson, J. A. K. Howard, *Chem. Commun.*, **1997**, 24, 2345–2346; c) J. R. Wigginton, S. J. Trepanier, R. McDonald, M. J. Ferguson, M. Cowie, *Organometallics*, **2005**, 24, 6194–6211; d) M.-E. Moret, D. Serra, A. Bach, P. Chen, *Angew. Chem., Int. Ed.*, **2010**, 49, 2873–2877.
- [8] J. C. Green, M. L. H. Green, G. Parkin, *Chem. Commun.* **2012**, 48, 11481–11503.
- [9] a) M. Brookhart, M. L. H. Green, *J. Organomet. Chem.*, **1983**, 250, 395–408; b) M. Brookhart, M. L. H. Malcolm, L. L. Wong, *Progr. Inorg. Chem.*, **1988**, 36, 1–124; c) W. Scherer, G. S. McGrady, *Angew. Chem. Int. Ed.*, **2004**, 43, 1782–1806; d) M. Brookhart, M. L. H. Green, G. Parkin, *Proc. Natl. Acad. Sci. USA*, **2007**, 104, 6908–6914; e) W. Scherer, V. Herz, A. Brück, C. Hauf, F. Reiner, S. Altmannshofer, D. Leusser, D. Stalke, *Angew. Chem. Int. Ed.*, **2011**, 50, 2845–2849; f) J. Sabmannshausen, *Dalton Trans.*, **2012**, 41, 1919–1923; g) M. Etienne, A. S. Weller, *Chem. Soc. Rev.*, **2014**, 43, 242–259.
- [10] a) F. A. Cotton, C. A. Murillo, R. A. Walton, in *Multiple Bonds between Metal Atoms*, 3rd. Ed, Springer Science And Business Media, Inc., New York, **2005**; b) M. H. Chisholm, N. J. Patmore in *Molecular Metal-Metal Bonds*, Chapter 6 (Ed.: S. T. Liddle), Wiley-VCH Verlag GmbH & Co. KGaA, Weinheim, **2015**.
- [11] D. H. Williamson, G. Wilkinson, *J. Am. Chem. Soc.* **1974**, 1079, 3824–3828.
- [12] a) R. A. Andersen, R. A. Jones, G. Wilkinson, *J. Chem. Soc. Dalton Trans.*, **1978**, 446–453; b) G. S. Girolami, V. V. Mainz, R. A. Andersen, *J. Am. Chem. Soc.*, **1981**, 103, 3953–3955; c) F. A. Cotton, K. J. Wiesinger, G. S. Girolami, V. V. Mainz, R. A. Andersen, *Inorg. Chem.*, **1990**, 29, 2594–2599.
- [13] J. H. Shin, G. Parkin, *Chem. Commun.* **1998**, 1273–1274.
- [14] a) M. E. García, A. Ramos, M. A. Ruiz, M. Lanfranchi, L. Marchio, *Organometallics*, **2007**, 26, 6197–6212; b) M. A. Alvarez, D. García-Vivó, M. E. García, M. E. Martínez, A. Ramos, M. A. Ruiz, *Organometallics*, **2008**, 27, 1973–1975; c) M. A. Alvarez, M. E. García, M. E. Martínez, A. Ramos, M. A. Ruiz, *Organometallics*, **2009**, 28, 6293–6307; d) M. A. Alvarez, M. E. García, M. E. Martínez, M. A. Ruiz, *Organometallics*, **2010**, 29, 904–916.
- [15] J.-G. Ma, Y. Aksu, L. J. Gregoriades, J. Sauer, M. Driess, *Dalt. Trans.* **2010**, 39, 103–106.
- [16] a) M. H. Chisholm, F. A. Cotton, M. W. Extine, C. A. Murillo, *Inorg. Chem.*, **1978**, 17, 2338–2340; b) M. H. Chisholm, J. C. Huffman, R. J. Tatz, *J. Am. Chem. Soc.*, **1983**, 105, 2075–2077.
- [17] a) M. Bochmann, in *Organometallics and Catalysis. An Introduction*, Oxford University Press, Oxford, UK, **2015**; b) J. F. Hartwig, in *Organotransition Metal Chemistry*, University Science Books, Casebound, **2010**; c) R. H. Crabtree, in *The Organometallic Chemistry of the Transition Metals*, 6th ed., John Wiley & Sons, Inc., Hoboken, **2014**; d) C. Elschenbroich, in *Organometallics*, 3rd ed., Wiley-VCH, Weinheim, **2006**.
- [18] a) G. J. Kubas, *J. Organomet. Chem.*, **2014**, 751, 33–49; b) S. Ogo, K. Ichikawa, T. Kishima, T. Matsumoto, H. Nakai, K. Kusaka, T. Ohhara, *Science*, **2013**, 339, 682–684; c) T. Liu, L. DuBois, R. M. Bullock, *Nat. Chem.*, **2013**, 5, 228–233; d) J. M. Camara, T. B. Rauchfuss, *Nat. Chem.*, **2011**, 4, 26–30; e) C. Tsay, J. C. Peters, *Chem. Sci.*, **2012**, 3, 1313–1318.
- [19] a) D. V. Yandulov, *Science*, **2003**, 301, 76–78; b) K. Arashiba, Y. Miyake, Y. Nishibayashi, *Nat. Chem.*, **2011**, 3, 120–125; c) J. A. Anderson, J. Rittle, J. C. Peters, *Nature*, **2013**, 501, 84–87.
- [20] a) T. Nguyen, A. D. Sutton, M. Brynda, J. C. Fetting, G. J. Long, P. P. Power, *Science*, **2005**, 310, 844–847; b) R. Wolf, C. Ni, T. Nguyen, M. Brynda, G. J. Long, A. D. Sutton, R. C. Fischer, J. C. Fetting, M. Hellman, L. Pu, P. P. Power, *Inorg. Chem.*, **2007**, 46, 11277–11290; c) C. Ni, B. D. Ellis, G. J. Long, P. P. Power, *Chem. Commun.*, **2009**, 17, 2332–2334.
- [21] a) N. V. S. Harisomayajula, A. K. Nair, Y.-C. Tsai, *Chem. Commun.*, **2014**, 50, 3391–3412; b) A. K. Nair, N. V. S. Harisomayajula, Y.-C. Tsai, *Inorg. Chim. Acta*, **2015**, 424, 51–62.
- [22] a) A. Noor, R. Kempe, *Inorganica Chim. Acta*, **2015**, 424, 75–82; b) C. Schwarzmaier, A. Noor, G. Glatz, M. Zabel, A. Y. Timoshkin, B. M. Cossairt, C. C. Cummins, R. Kempe, M. Scheer, *Angew. Chem. Int. Ed.* **2011**, 50, 7283–7286; c) A. Noor, G. Glatz, R. Müller, M. Kaupp, S. Demeshko, R. Kempe, *Nat. Chem.*, **2009**, 1, 322–325.
- [23] a) J. Shen, G. P. A. Yap, J.-P. Werner, K. H. Theopold, *Chem. Commun.*, **2011**, 47, 12191–12193; b) J. Shen, G. Yap, K. Theopold, *Chem. Commun.*, **2014**, 50, 2579–2581.
- [24] a) J. P. Krogman, C. M. Thomas, *Chem. Commun.*, **2014**, 50, 5115–5127; b) B. G. Cooper, J. W. Napoline, C. M. Thomas, *Cat. Rev. Sci. Eng.*, **2012**, 54, 1–40.
- [25] a) S. J. Terenjak, R. K. Carlson, L. J. Clouston, V. G. Young, E. Bill, R. Maurice, Y.-S. Chen, H. J. Kim, L. Gagliardi, C. C. Lu, *J. Am. Chem. Soc.*, **2014**, 136, 1842–1855; b) L. J. Clouston, R. B. Siedschlag, P. A. Rudd, N. Planas, S. Hu, A. D. Miller, L. Gagliardi, C. C. Lu, *J. Am. Chem. Soc.*, **2013**, 135, 13142–13148; c) R. J. Eisenhart, P. A. Rudd, N. Planas, D. W. Boyce, R. K. Carlson, W. B. Tolman, E. Bill, L. Gagliardi, C. C. Lu, *Inorg. Chem.*, **2015**, 54, 7579–7592.

- [26] a) M. Carrasco, N. Curado, E. Álvarez, C. Maya, R. Peloso, M. L. Poveda, A. Rodríguez, E. Ruiz, S. Álvarez, E. Carmona, *Chem. - A Eur. J.*, **2014**, *20*, 6092–6102; b) M. Carrasco, N. Curado, C. Maya, R. Peloso, A. Rodríguez, E. Ruiz, S. Álvarez, E. Carmona, *Angew. Chem. Int. Ed.*, **2013**, *52*, 3227–3231.
- [27] a) P. Siega, L. Randaccio, P. A. Marzilli, L. G. Marzilli, *Inorg. Chem.*, **2006**, *45*, 3359–68; b) C. A. Tolman, *Chem. Rev.* **1977**, 331–348
- [28] S. E. Kegley, A. R. Pinhas, in *Problems and Solutions in Organometallic Chemistry*, Oxford University Press, **1986**.
- [29] Y.-C. Tsai, Y.-M. Lin, J.-S. K. Yu, J.-K. Hwang, *J. Am. Chem. Soc.*, **2006**, *128*, 13980–13981.
- [30] a) T. G. Appleton, H. C. Clark, L. E. Manzer, *Coord. Chem. Rev.*, **1973**, *10*, 335–422; b) F. R. Hartley, *Chem. Soc. Rev.*, **1973**, *2*, 163–179; c) L. J. Manojlovic-Muir, K. W. Muir, *Inorg. Chim. Acta*, **1974**, *10*, 47–49; d) E. M. Shustorovich, M. A. Porai-Koshits, Y. A. Buslaev, *Coord. Chem. Rev.*, **1974**, *17*, 1–98; e) T. G. Appleton, M. A. Bennett, *Inorg. Chem.*, **1978**, *17*, 738–747; f) K. I. Purcell, J. C. Kotz, in *Inorganic Chemistry*, W. B. Saunders, Co. Philadelphia, **1977**, Chapter 13; g) J. C. Toledo, B. d. S. L. Neto, D. W. Franco, *Coord. Chem. Rev.*, **2005**, *249*, 419–431; h) J. Zhu, Z. Lin, T. B. Marder, *Inorg. Chem.*, **2005**, *44*, 9384–9390; i) S. G. Koller, R. Martín-Romo, J. S. Melero, V. P. Colquhoun, D. Schildbach, C. Strohmman, F. Villafañe, *Organometallics*, **2014**, *33*, 7329–7332.
- [31] a) M. A. Ortuño, P. Vidossich, G. Ujaque, S. Conejero, A. Lledós, *Dalton Trans.*, **2013**, *42*, 12165–12172; b) M. Etienne, J. E. MacGrady, F. Maseras, *Coord. Chem. Rev.*, **2009**, *253*, 635–646.
- [32] A. Falceto, K. H. Theopold, S. Alvarez, *Inorg. Chem.*, **2015**, *54*, 10966–10977.
- [33] Unpublished work from these laboratories.
- [34] a) S. F. Sousa, P. A. Fernandes, M. J. Ramos, *J. Phys. Chem. A* **2007**, *111*, 10439–10452; b) M. Linder, T. Brinck, *Phys. Chem. Chem. Phys.* **2013**, *15*, 5108–5114.
- [35] S. Horvath, S. I. Gorelsky, S. Gambarotta, I. Korobkov, *J. Am. Chem. Soc.*, **2008**, *47*, 9937–9940.
- [36] A. Noor, S. Schwarz, R. Kempe, *Organometallics* **2015**, *34*, 2122–2125.
- [37] B. E. Bursten, R. H. Cayton, *Organometallics*, **1986**, *47*, 1051–1053.
- [38] J. R. Torkelson, F. H. Antwi-Nsiah, R. McDonald, M. Cowie, J. G. Pruis, K. J. Jalkanen, R. L. DeKock, *J. Am. Chem. Soc.*, **1999**, *121*, 3666–3683.
- [39] G. M. Sheldrick, *Acta Cryst.* **2008**, *A64*, 112–122.
- [40] M. J. Frisch *et al.* (2009). Gaussian 09 (Revision A.1) Wallingford, CT.
- [41] A. D. Becke, *J. Chem. Phys.*, **1993**, *98*, 5648–56752.
- [42] A. Schäfer, C. Huber, R. Ahlrichs, *J. Chem. Phys.*, **1994**, *100*, 5829–5835.
- [43] R. Ahlrichs, K. May, *Phys. Chem. Chem. Phys.*, **2000**, *2*, 943–945.

WILEY-VCH

Accepted Manuscript